Fabrication of single crystalline gold nanobelts†‡

Ying Chen,[a] Cristoph Somsen,[b] Srdjan Milenkovic[a] and Achim Walter Hassel*[a]

Received 26th September 2008, Accepted 28th November 2008
First published as an Advance Article on the web 10th December 2008
DOI: 10.1039/b816897k

Well dispersed, single crystalline gold nanobelts, with unique {110} crystallographic facets, were synthesized by a combined method consisting of directional solid-state transformation of an Fe–Au eutectoid and a selective phase dissolution without the presence of any surfactant. They have an average thickness of 25–30 nm, a width of 200–250 nm, and an average length of 20 μm, exhibiting thus extremely high aspect ratios of more than 1500. The obtained gold nanobelts were characterized by field emission scanning electron microscopy, transmission electron microscopy, X-ray photoelectron spectroscopy, and UV-Vis spectrometry. The well-dispersed gold nanobelts can be selectively assembled onto substrates which have a significant potential for novel electrodes with a large effective surface area and a selective crystal orientation of {110}, less common for gold.

The reproducible preparation of nanocrystals with various shapes and exposed surfaces is of crucial importance for several applications of nanomaterials due to the anisotropic properties of crystals.[1–3] Spherical, planar and fibrous metal nanostructures, so called 3-, 2- and 1-dimensional nanostructures, have been intensively studied in the last two decades owing to their shape-dependent properties.[1,2,4,5] Particular interest has been focused on noble metals, such as Au, Ag and Cu, due to the fact that they are technologically important in many fields ranging from catalysis over optics and electronics to surface enhanced Raman spectroscopy (SERS).[6–9] Among various kinds of metal nanostructures, one dimensional (1-D) nanostructures such as nanowires, nanotubes, nanorods and nanobelts are particular interesting on account of their unique electrical and optical properties.[9–11] Nanobelts, the intermediate morphology between one and two dimensional, or one and half dimensional structures, have been intensively studied in the last few years, because they may be the ideal system for fully understanding dimensionally confined transport phenomena and building functional devices along individual nanobelts.[11,12] However, these studies were mainly focused on semiconductors, such as oxides[11] and sulfides,[13] whereas reports on the preparation of metal nanobelts, especially noble metal nanobelts, are scarce. A few examples were described in the literature, such as the preparation of Ag nanobelts by refluxing an aqueous silver colloidal dispersion[14] or by reduction of $AgNO_3$ with ascorbic acid in the presence of poly(acrylic acid) (PAA)[15] or the growth of Cu nanobelts on the surface of a TEM grid by a galvanic reduction.[16] Regarding gold nanobelts, only a few papers have been reported to date. Han *et al.*[17] synthesized gold nanobelts by a sonochemical method in the presence of glucose; Zhang *et al.*[18] reported the preparation of gold nanobelts *via* a one-dimensional self-assembly of triangular gold nanoplates with the help of PVP as capping agent; Zhao *et al.*[19] synthesized gold nanobelts and nanocombs in an aqueous mixed surfactant solution. Very recently, a novel approach[20] has been developed which is a simple and efficient method for the preparation of iso-oriented gold nanobelt arrays in an Fe matrix. It is based on a directional eutectoid transformation followed by a selective phase electrochemical dissolution of the Fe. These gold nanobelts are prepared by a combination of a metallurgical process step with a subsequent selective dissolution that is either chemically or electrochemically performed. This method of synthesis allows for control of the crystallographic properties and size features. Specific applications including NEMS (nanoelectromechanical systems),[21] chemical or electrochemical sensors[9] may be considered based on this synthesis making use of the advantageous single crystallinity.

It is very interesting to fabricate gold nanostructures with various morphologies, which may be the building blocks for nanodevices. Herein, as a consequence, gold nanobelts were extracted from the matrix and a well dispersed suspension was obtained by phase selective chemical dissolution in the absence of surfactant. By choosing the solvent carefully, well-dispersed gold nanobelts were obtained, which enable the self-assembly of gold nanobelts on the intended patterned substrates for electronic applications. To get one dimensional structures by using directional eutectic/eutectoid transformation, a binary system showing eutectic like reaction with gold as the minor phase must be selected. Our previous studies[20,22] and the existing data[23] confirmed that, interestingly, only the Fe–Au system shows this characteristic, where a eutectoid reaction takes place at 868 °C and 2.3 at.% Au. Pre-alloys were prepared using 99.999% Au and 5-times zone-refined Fe, by induction melting under an Ar atmosphere and drop casting into a cylindrical copper mould. After subsequent fitting into alumina crucibles, samples were directionally transformed in a Bridgman type solidification furnace with resistance heating. The details were described elsewhere.[22] Afterwards, the samples were cut into $1 \times 1 \times 0.1$ cm^3 pieces and ground for further treatment. The selective dissolution of the α-Fe phase in the eutectoid alloy was achieved through selective chemical etching in 1.0 M HNO_3 with the presence of 0.05 M *o*-phenanthroline as a chelating agent to prevent the hydrolysis of Fe ions during the dissolution process. Phenanthroline was chosen because it has a strong chelating effect even under acidic conditions. The reaction was continued for two hours to make sure that the entire solid sample was dissolved in the etching solution, and stirring was applied throughout the entire process to reduce the possible coagulating tendency of gold nanobelts. The samples were

[a]*Max-Planck-Institut für Eisenforschung GmbH, Max-Planck-Str. 1, D-40237 Düsseldorf, Germany. E-mail: hassel@elchem.de; Fax: +49 211 6792 218*
[b]*Institute of Materials, Department of Mechanical Engineering, Ruhr-University Bochum, Universitätsstr. 150, D-44780 Bochum, Germany*
† This paper is part of a *Journal of Materials Chemistry* theme issue on Nanotubes and Nanowires. Guest editor: Z. L. Wang
‡ Electronic supplementary information (ESI) available: XPS of iron, XRD and EDX-elemental mapping. See DOI: 10.1039/b816897k

first separated by centrifugation, then washed with water in an ultrasonic bath, and once again separated by centrifugation to remove the remaining acid and Fe ions. This procedure was repeated several times until the pH value of the final solution was 7.0. Finally, the products were dispersed in isopropyl alcohol (IPA) under ultrasonication to obtain suspensions for further characterization.

The morphology of the precipitate was characterized by field emission scanning electron microscopy (FE-SEM, LEO 1550VP, GEMINI). As shown in Fig. 1, the low magnification image (Fig. 1a) indicates that the products consist of a large amount of gold nanobelts that are well dispersed. The higher magnification image (Fig. 1b) clearly reveals that the nanobelts are tens of micrometers long and 250–300 nm wide. The thickness, obtained by measuring the distance between two facets of a belt lying on the silicon substrate, is about 25–30 nm (see Fig. 1c). As seen from the FE-SEM images, the nanobelts are uniform in both lateral (250–300 nm) and longitudinal dimensions (20–25 μm). The lateral dimension change can be clearly seen from the bending at the end or the centre of one nanobelt as seen from FE-SEM (Fig. 1d) and TEM (Fig. 1e) images, which is a clear evidence of a belt morphology. Moreover, some of the nanobelts can be more than 50 μm long, as shown in Fig. 1f. Considering that the thickness is only about 25–30 nm, the aspect ratio is more than two thousand. Small quantities of short nanobelts were also observed as by-products, as can be seen in Fig. 2a; this is mainly due to the ultrasonication process, which may break some of the long nanobelts considering the high oscillation energy and the extremely high aspect ratio.

Transmission electron microscopy (TEM) further reveals the morphology and the detailed structure of the obtained gold nanobelts. Fig. 2a and b show that the belt-like gold structures are well dispersed. Also, one can clearly see that the width of the nanobelts is about 250–300 nm and the length can be several tens of micrometers. Furthermore, the band-like patterns shown on the surface of the nanobelts in Fig. 2b are due to deformation or bending of the nanobelt during the irradiation of the electron beam, which is frequently observed in metal foils.[5,24] To further characterize the crystallographic structure of the nanobelts, the high resolution transmission electron microscopy (HRTEM) image and the corresponding selected-area electron diffraction (SAED) pattern were obtained by focusing the electron beam perpendicular to a nanobelt lying flat on the support carbon film, as shown in Fig. 2c and d. The measured interplanar spacing along the growth direction of gold nanobelts is 0.235 nm, which corresponds to the (111) lattice plane of the face-centred-cubic (fcc) gold. Fig. 2d presents the SAED pattern of gold nanobelts, which was obtained by focusing the electron beam on a nanobelt lying flat on TEM grid. In contrast to the reported results,[17–19] hexagonal symmetry was not generated. The measured results demonstrate that the gold nanobelt is a single crystal and the lateral facets of the nanobelt are presented by {110} planes. The SAED patterns are essentially identical over the entire belt, which proved the single-crystallinity and structurally uniform nature of the nanobelts. The unique chemical and physical properties of nanocrystals are determined not only by the size of the particles but also by the particle shape. Both the surface atoms and the surface crystallographic structures of the particle will determine the properties of nanocrystals.[2] The {111}, {100}, and possibly {110} surfaces of fcc structured metal nanoparticles, for example, are different not only in the surface atom densities but also in the electronic structure, bonding, and possibly chemical reactivities.[2] For thin fcc metal foils, such as nanoplates and nanobelts, the {110} surfaces are rarely seen,[17–19,24] due to their high surface free energy compared to that of {111} and {100} surfaces. Recently, Zhang *et al.*[25] and Diao *et al.*[26] investigated the reorientation of gold nanobelts by means of molecular dynamics simulation (MDS) with the embedded atom method. The simulation results demonstrated that the surface stress induces reorientation

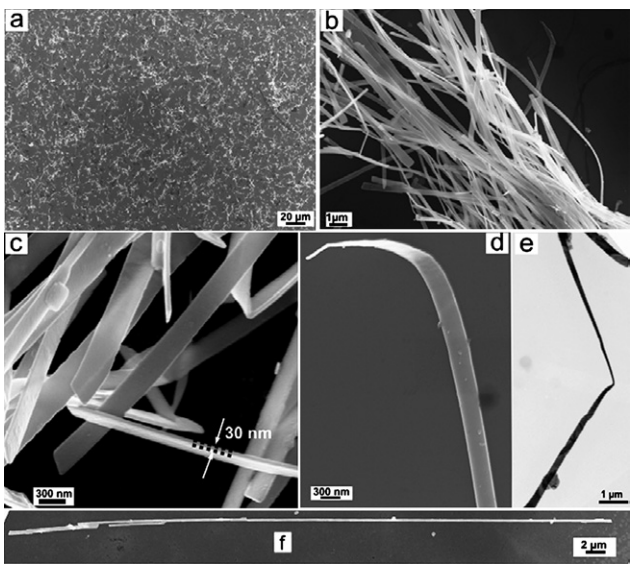

Fig. 1 a) Low and b) high magnification FE-SEM images of the obtained gold nanobelts dispersed in IPA; c) the thickness of gold nanobelt; d) FE-SEM and e) TEM images show the change in lateral dimension within one nanobelt; f) the length of one typical, long nanobelt.

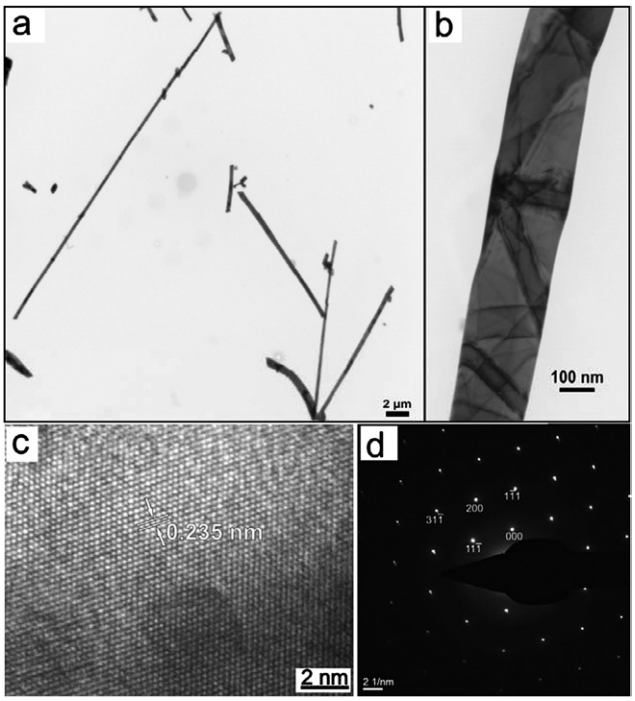

Fig. 2 TEM images with a) low and b) high magnification of gold nanobelts dispersed in IPA; c) HRTEM image, and d) the corresponding SAED pattern of a single gold nanobelt.

from a <100> gold nanobelt into an fcc <110> belt and that the structural stability of Au nanobelts depend on size, initial orientation and temperature. However, these simulations consider unsuspended surfaces of the belts during their growth, which is quite different from the case presented here, where gold nanobelts grow cooperatively and concurrently with the iron matrix. During a eutectoid decomposition, phases usually develop a certain crystallographic orientation relationship during the growth in order to minimize overall interface energy. The crystallographic orientation relationship depends on the crystal structures of the phases and the lattice parameter ratio. For the Fe–Au system it has been shown that the energetically most favourable crystallographic orientation of nanobelts is {110}.[27] This unique surfaces of the gold nanobelts synthesized here, combined with the reported gold nanobelts,[17–19] could enable the study of anisotropic properties of nanostructures taking advantage of the gold nanobelts prepared with different methods having a similar morphology but different atomic arrangement on the surface. For example, the chemical reactivity of different surfaces could be different[3,27,28] and the difference of the absorption abilities of molecules on {111} and {110} surfaces could be quantitatively detected by using SERS[30] or electrochemistry.[31] Avramov-Ivic *et al.*[32] found that the electro-catalytic oxidation of some organic compounds, such as methanol, on the {110} surface is more favourable than on the other two low index planes. This could be one of the benefits of the unique {110} Au nanobelts compared with the previously reported 'normal' {111} Au nanobelts. And, very recently, Xiang *et al.*[33] reported that tuning of the morphology of Au nanorods is possible by switching the growth tendency of {110} facets from restriction to preference through changing the concentration of capping agent during the anisotropic growth process, which could be utilised for tuning the morphology of Au nanobelts in the present case due to the large {110} surfaces. The formation of unstable {110} facets originates from a crystallographic orientation relationship between the gold nanobelts and the iron matrix established during directional eutectoid decomposition[27] at high temperature.

The chemical composition of the belts was determined by X-ray photoelectron spectroscopy (XPS, Physical Electronics Quantum 2000 Scanning ESCA Microprobe, sputtering 2 keV Ar^+). The XPS results (Fig. 3a) show that the gold nanobelts are pure metallic gold, which can be confirmed from the binding energy for Au $4f_{7/2}$ located at 84 eV; and there is no signal of the possible impurity from Fe. The X-ray diffraction (XRD) pattern provides further support for the characteristic of face-centered cubic (fcc) Au. Additionally, the FE-SEM and EDX-elemental mapping investigations confirmed the iron-free gold nanobelts (for XPS of iron, XRD and EDX-elemental mapping, see ESI†).

Optical properties of gold nanomaterials are strongly influenced by the particle shape and size as a result of surface plasmon resonance (SPR). Suspensions of small spherical gold nanoparticles show amaranth to red colour owing to SPR and exhibit a single absorption band, which is located at about 520 nm or longer wavelengths when the size is increasing. For the 1-D nanomaterials, there are two surface plasmon resonance absorption peaks which are characteristic of short (transverse band) and long (longitudinal band) axes of these systems.[3] Fig. 3b shows the UV-Vis spectrum of gold nanobelts dispersed in IPA. The same as the reported results,[17–19] gold nanobelts here also have two surface plasmon resonance absorption peaks. The first one is located at about 540 nm, corresponding to the short axes of the gold nanobelts; and the other one is located in the range from

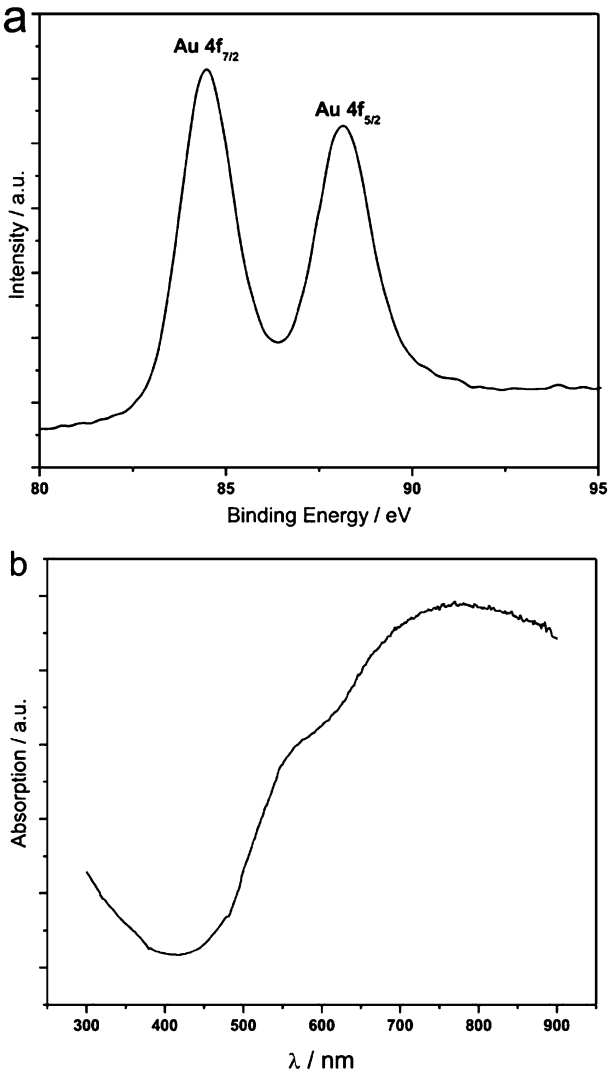

Fig. 3 a) XPS of gold nanobelts, the binding energy value is 84 eV for Au $4f_{7/2}$ which coincides with that of Au^0. b) UV/Vis spectrum of gold nanobelts dispersed in IPA.

780 to 900 nm, contributed from the longitudinal SPR absorption of the long axes of the nanobelts. As mentioned above, some short nanobelts always appeared as by-products. The peak from the long axes of these short nanobelts is quite broad, so that the peak from the short axes shows only a weak shoulder peak.

In summary, high aspect ratio, single crystalline Au nanobelts with unique {110} facets were successfully synthesized through a combined method of directional solid state decomposition of an Fe–Au eutectoid and a selective phase dissolution process. The method is simple, convenient, economical and easily applicable at a large scale (gram scale). Moreover it can be easily used in functional electronics, optoelectronics or sensing devices by assembling the Au nanobelts onto the functionalized surfaces of different substrates.

Acknowledgements

Ying Chen acknowledges International Max-Planck Research School (IMPRS) – SurMat for financial support through

a fellowship. The financial support of the Deutsche-Forschungs-Gemeinschaft through the project Functional Devices from Directionally Grown Nanowire Arrays HA 3118/4-3 within the DFG Priority Programme 1165 Nanowires and Nanotubes – From Controlled Synthesis to Function is gratefully acknowledged.

Notes and references

1 C. Burda, X. Chen, R. Narayanan and M. A. El-Sayed, *Chem. Rev.*, 2005, **105**, 1025.
2 Z. Wang, *J. Phys. Chem. B*, 2000, **104**, 23.
3 C. J. Murphy, T. K. San, A. M. Gole, C. J. Orendorff, J. X. Gao, L. Gou, S. E. Hunyadi and T. Li, *J. Phys. Chem. B*, 2005, **109**, 13857.
4 B. Wiley, Y. Sun, B. Mayers and Y. Xia, *Chem. Eur. J.*, 2004, **11**, 454.
5 J. U. Kim, S. H. Cha, K. Shin, J. Y. Jho and J. C. Lee, *Adv. Mater.*, 2004, **16**, 459.
6 C. J. Murphy, *Science*, 2002, **298**, 2139.
7 R. C. Jin, Y. W. Cao, C. A. Mirkin, K. L. Kelly, G. C. Schatz and J. G. Zheng, *Science*, 2001, **294**, 1901.
8 Z. Q. Tian, B. Ren and D. Y. Wu, *J. Phys. Chem. B*, 2002, **106**, 9463.
9 C. J. Murphy, A. M. Gole, S. E. Hunyadi, J. W. Stone, P. N. Sisco, A. Alkilany, B. E. Kinard and P. Hankins, *Chem. Commun.*, 2008, 544.
10 Y. N. Xia, P. D. Yang, Y. G. Sun, Y. Y. Wu, B. Mayers, B. Gates, Y. D. Yin, F. Kim and Y. Q. Yan, *Adv. Mater.*, 2003, **15**, 353.
11 Z. W. Pan, Z. R. Dai and Z. L. Wang, *Science*, 2001, **291**, 1947.
12 *Nanowires and Nanobelts: Materials, Properties, and Devices*; Z. L. Wang, Kluwer Academic Publishers: Norwell, MA, 2003.
13 Y. C. Zhu, Y. Bando and D. F. Xue, *Appl. Phys. Lett.*, 2003, **82**, 1769.
14 Y. G. Sun, B. Mayers and Y. N. Xia, *Nano Lett.*, 2003, **3**, 675.
15 J. W. Bai, Y. Qin, C. Y. Jiang and L. M. Qi, *Chem. Mater.*, 2007, **19**, 3367.
16 T. K. Huang, T. H. Cheng, M. Y. Yen, W. H. Hsiao, L. S. Wang, F. R. Chen, J. J. Kai, C. Y. Lee and H. T. Chiu, *Langmuir*, 2007, **23**, 5722.
17 J. L. Zhang, J. M. Du, B. X. Han, Z. M. Liu, T. Jiang and Z. F. Zhang, *Angew. Chem. Int. Ed.*, 2006, **45**, 1116.
18 J. Zhang, H. Liu, Z. Wang and N. Ming, *Appl. Phys. Lett.*, 2007, **91**, 3.
19 N. Zhao, Y. Wei, N. Sun, Q. Chen, J. Bai, L. Zhou, Y. Qin, M. Li and L. Qi, *Langmuir*, 2008, **24**, 991.
20 Y. Chen, S. Milenkovic and A. W. Hassel, *Nano Lett.*, 2008, **8**, 737.
21 V. Cimalla, C. C. Röhlig, J. Pezoldt, M. Niebelschütz, O. Ambacher, K. Brückner, M. Hein, J. Weber, S. Milenkovic, A. J. Smith and A. W. Hassel, *J. Nanomater.*, 2008, **2008**, 638947.
22 S. Milenkovic, A. Schneider and A. W. Hassel, *Gold Bull.*, 2006, **39**, 185.
23 E. Isaac and P. Z. Walter, *Anorg. Metallkd.*, 1950, **41**, 234.
24 Y. Chen, X. Gu, C. G. Nie, Z. Y. Jiang, Z. X. Xie and C. J. Lin, *Chem. Commun.*, 2005, 4181.
25 C.-F. Zhang, H.-L. Wei, J. Wang and L.-Z. Liu, *Chinese Phys. Lett.*, 2007, **24**, 2227.
26 J. Diao, K. Gall and M. L. Dunn, *Phys. Rev. B*, 2004, **70**, 075413.
27 S. Milenkovic, T. Nakayama, M. Rohwerder and A. W. Hassel, *J. Cryst. Growth*, DOI: 10.1016/j.jcrysgro.2008.10.022.
28 N. R. Jana, L. Gearheart, S. O. Obare and C. J. Murphy, *Langmuir*, 2002, **18**, 922.
29 T. Mokari, E. Rothenberg, I. Popov, R. Costi and U. Banin, *Science*, 2004, **304**, 1787.
30 N. R. Jana and T. Pal, *Adv. Mater.*, 2007, **19**, 1761.
31 J. Hernández, J. Solla-Gullón, E. Herrero, A. Aldaz and J. M. Feliu, *J. Phys. Chem. B*, 2005, **109**, 12651.
32 M. Avramov-Ivić, V. Jovanović, G. Vlajnić and J. Popić, *J. Electroanal. Chem.*, 1997, **423**, 119.
33 Y. Xiang, X. Wu, D. Liu, L. Feng, K. Zhang, W. Chu, W. Zhou and S. Xie, *J. Phys. Chem. C*, 2008, **112**, 3203.